Finite Element Analysis of Reinforced Concrete Deep Beams

Muhammed M. Ahmed Sarkawt A. Hasan*

College of Engineering, University of Salahaddin, Arbil
Kurdistan Region, Iraq

ABSTRACT

The nonlinear analysis of reinforced concrete deep beams using finite element method is presented here. The nonlinearity included the nonlinear behavior, anisotropy under biaxial state of stress, cracking and crushing of concrete. The post cracking shear transfer in concrete by aggregate interlock and yielding of reinforcement are also considered in the analysis.

A quadrilateral eight-noded isoparametric elements were used to represent concrete materials, while bar elements perfectly connected to the concrete nodes were used to represent the steel.

Validity of the proposed model was checked by analysis of three reinforced concrete deep beams. The results showed good agreement with experimental ones.

Deep beams with openings of different sizes and locations were also analyzed. The results showed that proposed model can represent effects of the openings on behavior of deep beams including ultimate load capacity, crack propagation, stress and strain 4

* Part of his M.Sc. Thesis

1. Introduction

The usual analysis methods in ordinary beams can not be applied to deep beams because this type of beams have a significant shear deformations and vertical normal stresses. Reinforced concrete is a nonlinear material, this nonlinearity introduces several complexities in the analysis, therefore classical method, which describes the problem with partial differential equations is difficult if not impossible. The finite element method as a numerical technique offers a rigorous and rational analysis of reinforced concrete structures especially deep beams.

The earlier studies in using finite element method in the analysis of reinforced concrete structures were made by Ngo and Scordelie (3) in 1967, Nilson (4) in 1968, Valliappan and Doolan (5) in 1972, Robins and Kong (6) in 1973, Suidan and Schnobrich (7) in 1973, and others.

Analysis of reinforced concrete deep beams by finite element method was studied by Robins and Kong (6) in 1973, Cope and Rao (10) in 1977, Phillips and Zienkiewicz (9) in 1976, Gogate and Bishara (12) in 1980, and Mahmood (13) in 1986. In these studies several models were made to represent the reinforced concrete material. In the last study (13), the concrete was represented by linear isoparametric elements or quadrilateral elements with incompatible mode. The main steel was represented by bar or constant strain triangular elements. Linkage elements with proper stiffness were presented to simulate the interaction between main steel and concrete. The secondary steel was represented by bar elements and perfect bond was assumed between concrete and secondary steel. The stress-strain relationship for concrete was taken to be linear as givin by Liu (17) in compression, while in tension the relationship was considered to be nonlinear in certain ranges of stress ratios. The incremental iterative procedure with variable stiffness matrix was adopted in the nonlinear solution algorithm.

The present work aims to develop a simple behavioral model, applied to finite element program, capable of modeling the nonlinear behavior of plain reinforced concrete deep beams under monotonic loading up to failure.

2. Material Constitutive Relationship

2.1 Concrete constitutive relationship

2.1.1 Biaxial stress-strain relation for concrete

For nonlinear elastic homogenous, and isotropic material, the equation:

$$f = \frac{e * E}{(1 - v\,k)} \quad \ldots\ldots (1)$$

Is applicable as a biaxial stress-strain relation, where "f" is the principle stress in any direction; "e" is the strain in that direction' "E" is the modulus of elasticity; "v" is the poisson's ratio, and "k" is the ratio of stress in the orthogonal direction to the principal stress in the direction considered.

An expression similar to Equ. (1). Modified to account for the nonlinear nature of concrete under biaxial compression, as proposed by Liu (17):

$$f = \frac{e * E}{(1-v\,k)\left(1+\left(\frac{1}{1-v\,k} * \frac{E}{Es} - 2\right)\left(\frac{e}{ep}\right)+\left(\frac{e}{ep}\right)^2\right)} \quad \ldots\ldots\ldots (2).$$

Where Es = fp / ep

fp : peak stress in biaxial compression.

ep : peak strain in biaxial compression.

3- For biaxial tension – tension :

Major direction fp1 = ft
Minor direction fp2 = k1 * fp1..... (8)
K1 = f2 / f1 k2 = f1 / f2 ..... (9)

f1 , f2 : stress in principal directions 1 and 2, respectively.

fp1 , fp2 : peak stress in principal directions 1 and 2, respectively.

B- Strain at Peak Stress Under Biaxial Stress

Based on the experimental work of Kupfer et al (15), Mahmood (13) proposed the following relations for determining the values of peak strains:

(1) In compression-compression zones:
(a)In major direction:

$$ep = -2200 - 25.45\ B$$
$$\text{For } 0^o <= B <= 27.5^o$$
$$ep = -3685.67 + 28.57\ B$$
$$\text{For } 27.5^o < B <= 45^o \quad ..... (10)$$

(b)In the minor direction:

$$ep = 770 - 56\ B$$
$$\text{For } 0^o <= B <= 27.5^o$$
$$ep = 1800 - 93.14\ B$$
$$\text{For } 27.5^o < B <= 45^o \quad ...(11)$$

where $B = \tan^{-1}(f1/f2)$

(2) In compression-tension zone:

(a) In compression:

$$ep = -2200 + 173.8\ B$$
$$\text{For } 0^o <= B <= 7.5^o$$
$$ep = -980 + 10.6\ B$$
$$\text{For } 7.5^o < B <= 90^o \quad ..... (12)$$

(b) In tension:

$$ep = 770 - 62.67\ B$$
$$\text{For } 0^o <= B <= 7.5^o$$
$$ep = 317 - 2.3\ B$$
$$\text{For } 7.5^o < B <= 90^o \quad .....(13)$$

where $B = \tan^{-1}(f1/-f2)$

(3) In tension-tension:

(a) In the major direction:

$$ep = 110 - 0.777\ B \quad ..... (14)$$

(b) In the minor direction:

$$ep = -26 + 2.24\ B \quad ..... (15)$$

where $B = \tan^{-1}(f2/f1)$

In the present investigation Eqns.(10) to (15) were used for obtaining values of peak strain.

2.1.2 Biaxial Orthotropic Constitutive Relation for Concrete

Liu (18) derived an orthotropic constitutive relation in matrix form, suitable for use in finite element analysis, as follows:

$$\begin{vmatrix} f1 \\ f2 \\ f12 \end{vmatrix} = \begin{vmatrix} \frac{E1}{E2}\lambda & \nu\lambda & 0 \\ \nu\lambda & \lambda s & 0 \\ 0 & 0 & \frac{E1'\ E2'}{E1' + E2' + 2E2'\nu} \end{vmatrix} * \begin{vmatrix} e1 \\ e2 \\ e1 \end{vmatrix} \quad \ldots\ldots (16)$$

In which the stresses and strains are listed In order of maximum, minimum and shear.

$\lambda = El' / [(El' / E2') - v^2]$

$Ei = Ei' / (1 - V Ki)$

Where Ei can be obtained by differentiating Eqn.(2) with respect to " e " as follows:

$$Ei = \frac{E\left[1 - \left(\frac{ei}{epi}\right)^2\right]}{(1-\nu ki)\left[1+\left(\frac{1}{1-\nu ki} * \frac{E}{Esi} - 2\right)\left(\frac{ei}{epi}\right) + \left(\frac{ei}{epi}\right)^2\right]} \quad \ldots\ldots\ldots (17)$$

in which $Esi = fpi / epi \qquad i = 1, 2$

The relation (16) was proposed by Liu [181 to represent orthotropic constitutive relation for concrete under biaxial compression stress. In the present investigation this relation has also been used for other states of stress.

2.1.3 Appliance of Stress- Strain Relationships

Based on stress-strain curves of concrete obtained by Kupfer [151 in 1969, Mahmood [13] in 1986 assumed that the concrete behaved linearly in tension up to a value of 60 % of the peak stress in both biaxial tension and in biaxial compression-tension for stress ratio k2 = f1 / f2 in the range $(-0.2 > k2 > -\infty)$. After this limited stress value the relation was considered nonlinear and Eqn.(2) was used. For other stress ratios in biaxial compression-tension zone. and for biaxial compression zone the relation considered nonlinear according to Eqn.(2).

2.2 Shear Modulus for Cracked Concrete

Cracked concrete element is considered capable of carrying some shear components by aggregate interlock phenomena. Celodin et al [11] suggested a linear degradation in the shear modulus of cracked element with strain normal to crack direction as follows:

$G'=F*(1-el/ec)*E; 0<el<ec \quad \ldots\ldots\ldots (18)$

$G' = 0 \quad ; el > ec$

In which G' = reduced shear modulus; F = numerical constant; e1 = fictitious strain in the direction normal to the crack; ec = limiting strain value after which aggregate interlock becomes zero. For shallow beams, it was found [ll] that value of F=0.1, and ec = 0.0045 give good results, while for deep beams. value of F = 0.3 and ec = 0.0022 was found [13] to give good results.

2.3 Failure criteria

2.3.1 Tension-Tension

When the major principal stress or strain exceeds its limiting value in Eqn.(8) and (14). a tension crack is assumed to develop in direction normal to that of major principal direction. This cranking model is known as a "smeared crack model" where an infinite number of parallel fissures were assumed to take place across that part of the isoparametric element represented by an integration point (Fig.1). When the crack occurs in the major principal direction the stiffness of the material in that direction is set to zero, and the constitutive relation (16) is reduced to:

$$\begin{vmatrix} f1 \\ f2 \\ f12 \end{vmatrix} = \begin{vmatrix} 0 & 0 & 0 \\ 0 & E2 & 0 \\ 0 & 0 & G' \end{vmatrix} * \begin{vmatrix} e1 \\ e2 \\ e3 \end{vmatrix}$$

Where - E2 - is the uniaxial modulus of elasticity in the minor principal direction. obtained from Eqn.(17) by setting value of stress ratio to zero, and " G' " is given in Eqn.(18).

2.3.2 Compression-Tension

When the positive principal stress " fi " or strain " el " exceeds the corresponding limiting value given in Eqns.(7) and (13), a crack was assumed to take place. " El " Is set to zero, and " G " Is reduced to " G' ".

2.3.3 Compression-Compression

When the major principal strain exceeds Its limiting value given by Eqn.(10), a crushing is assumed to occur. Also " El ", " E2 " and " G " are all set to zero.

2.4 Constitutive Relation Transformation

The constitutive relations in Eqns.(16) and (19) are functions of the principal stress and the principal strain values. These relations are referred to the principal axes, therefore, for stiffness calculation, it is necessary to transform such relations into global axes using the transformation relation:

$$[D] = [T]^T [D'] [T] \quad \ldots\ldots (20)$$

Where

$$[T] = \begin{vmatrix} C & S & cs \\ s & c & -cs \\ -2cs & 2cs & c - s \end{vmatrix} \{ e \} \quad \ldots\ldots (21)$$

$c = \cos B \quad s = \sin B$

B is the counterclockwise angle between general global coordinates that coincide with principal axes.

[D'] is the constitutive matrix for element in principal direction

[D] is the constitutive matrix for element in global coordinates **X, Y.**

2.5 Steel

In this investigation. steel was assumed to be linear elastic-perfectly plastic material

2.6 Steel-Concrete Interaction

Bond is the phenomenon of stress transfer between steel and concrete. Since the tensile strength of_concrete is usually considered to be more critical than the bond strength [14] and because the linakage element provided by Ngo and Scordelis and Nilson is based only on certain assumptions [5], therefore in this investigation the perfect bond was assumed to simulate the interaction between steel and concrete.

3 - Finite Element Idealization

Quadrilateral isoparametric eight-noded elements with 2 x 2 integraion Gauss points [Fig.2] are used to represent the concrete. Bar elements perfectly connected to concrete nodes are used to represent both main and secondary steel. The supports are represented by using 2-Dimensional constant strain triangular elements. The characteristics of these elements types are presented in many text books (31.22.23.24).

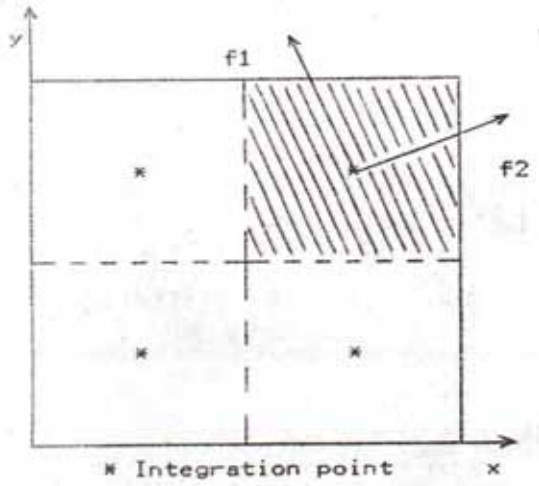

Fig. (1) Smeared – cracking model.

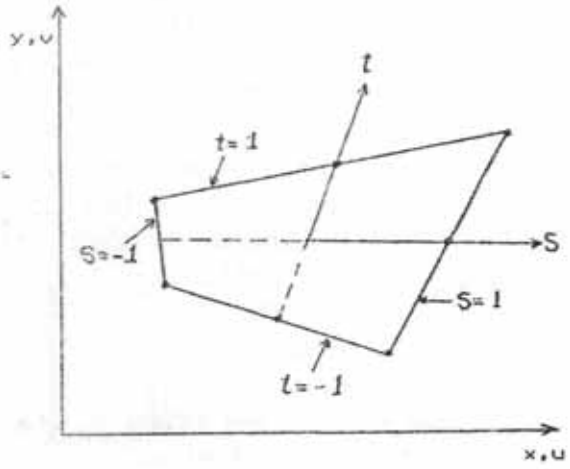

Fig. (2) Quadri Lateral Isoparametric element..

4 - Nonlinear Soluton

4.1 Nonlinear Solution Technique

The combined incremental-iteration method is utilized, in which the model are loaded incrementally with preselected load Increment. And for each increment a successive iterations are made to improve the equilibrium of the structure.

4.2 Nonlinear solution algorithm

The nonlinear algorithm solution steps are given below and the flow chart of the algorithm is given in the next pages:

1- At the beginning of first increment. The tangential stiffness matrix [Kt] is formed and assembled using initial material properties.

2- First load increment is formed.

3- Incremental displacement $\{\Delta u^i\}$ are calculated:

$$(\Delta u^i) = [Kt^{i-1}]^{-1} * (\Delta p^i) \quad \text{.....(22)}$$

Where $[\Delta p^i]$ is the incremental load Vector, $[Kt^{i-1}]$ is the tangential global stiffness matrix.

4-Total, displacement $[u^i]$ are calculate by adding the current incremental displacements (Δu^i) to the previous accumulative incremental displacements $[u^{i-1}]$.

4- Using the incremental displacements $[\Delta U^i]$, incremental strains $\{\Delta e^i\}$ are calculated:

$$\{\Delta e^i\} = [B]\ (\Delta u^i) \quad \text{.....(23)}$$

where [B] is the strain-displacement relationship matrix.

5- The incremental strains $\{\Delta e^i\}$ are added to the previous accumulative strains (e^{i-1}) to obtain total strain $\{e^i\}$.

6- Principal strains are calculated from the total strains $\{e^i\}$.

7- From the principal strains, principal stresses are calculated using Eqn.(2)

8- The cracking and crashing in concrete are checked.

9- The stress in steel are calculated.

10- The yielding in steel is checked.

11-According to the current material roperties, a new tangential global stiffness natrix [Kt] is formed and assembled.

12-Unbalanced forces are calculated from the difference between the applied load and the actual resulting forces in the structure.

13-The steps 3-12 are repeated until the convergence criteria is satisfied or number of iterations is exhausted. For this repeatation process, unbalanced forces calculated in step 12, and tangential global stiffness" matrix calculated in step 13 are used in the analysis.

14-A new load increment is formed and the steps 3-15 are repeated.

It should be noticed that the tangential global stiffness matrix is not constant through the iteration procedure for each load

increment. where it is recalculated in each iteration in order to increase the convergence rate.

In the above algorithm " i " denotes iterative number. where the numbering process starts from the first iteration in the first load Increment, and continues throughout the subsequent load increments.

Unbalanced forces :

It is calculated at the end of iteration " i " according to the following relation [13]:

$[UP^i] = (1 - \theta)[(\Delta p^i) - [Kt^i]\{\Delta u^i\}]$ .....(24)

Where $\{\Delta pi\}$ Is the applied load In this iteration; $\{\Delta u^i\}$ is the incremental displacements calculated according to Eqn.(22) by using the tangential global stiffness matrix at the end of last iteration $[Kt^{i-1}]$. θ is a constant was taken equal to 0.5 to minimize the truncation error.

Convergence criteria:

In this Investigation the following convergence criteria which is used by Philips and Zienkiewicz et al [9] is used:

$CF = (\{Up\}^T\{Up\})^{1/2}/(\{P\}^T\{P\})^{1/2}$..... (25)

This equation represent the ratio of norm of unbalanced forces to the norm applied load. CF is a pre selected convergence factor and it was taken in the range of (0.01-0.02).

5 - Results and Discussion

5.1 Reinforced Concrete Deep Beams Without Openings

The developed analytical model - F.E program was checked by solving three deep beams of different span-depth ratio tested experimentally by Kong et al [8] and analyzed numerically by Mahmood [13]. the geometry and reinforcement of these beams are shown in Fig. (3). All beams have width of section equal to 76.2 mm. The notation of the beams are the same as originally given by Kong [8]. The main reinforcement consist of one steel bar of 19.1 mm diameter of 286 MPa average yield strength. The web reinforcement consist of 7.9 mm and 9.5 mm diameter of 300 MPa and 280 MPa average yeild strength. respectively.

The ultimate uniaxial compressive strength (fc') and the cylinder splitting tensile (fsp) of concrete for the three beams are as shown below:

Table (1) Details of the beams tested by Kong [10]

Properties	Beam No.		
	3-10	1-20	4-30
fc' (MPa)	22.5	21.0	23.5
fsp(MPa)	2.69	2.76	2.6

5.1.1Finite Element Idealization

Due to the symmetry in both geometry and loading one half of the beams is analyzed by preventing the nodal points along the centerline from moving in horizontal direction. While they were allowed to be free to move in vertical direction (Fig.(4)). The concrete is idealized by using 15, 20 and 25 quadrilateral isoparametric eight-node elements for the beams 3-10, 1-20 and 4--30, respectively. Where in all these 5 elements are used along the half span, with 3, 4 and 5 elements along the depth for beams 3-10, 1-20 and 3-40,respectlvely. Both main and secondary steel are idealized by bar elements assumed perfectly connected to the nodes. The support is idealized by using four triangular elements of steel having thickness equal to the thickness of the base plate and width equal to the width of the beams.

In the analytical solution of ordinary beams, some of the previous investigations (25.25,27) ignored cover of the tension reinforcement in order to simplify the finite element solution, and because deep beams have ratio of cover to overall depth much smaller than that of ordinary beams, therefore tension cover is also ignored in the present idealization.

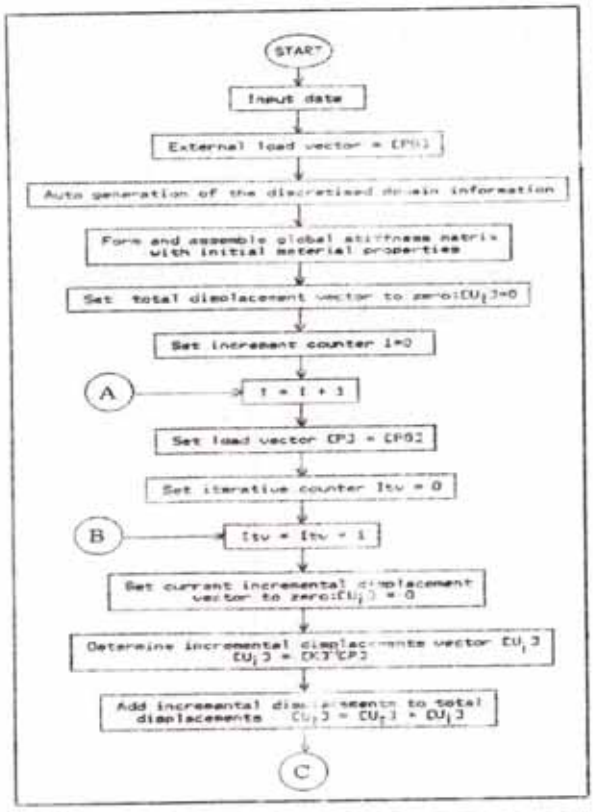

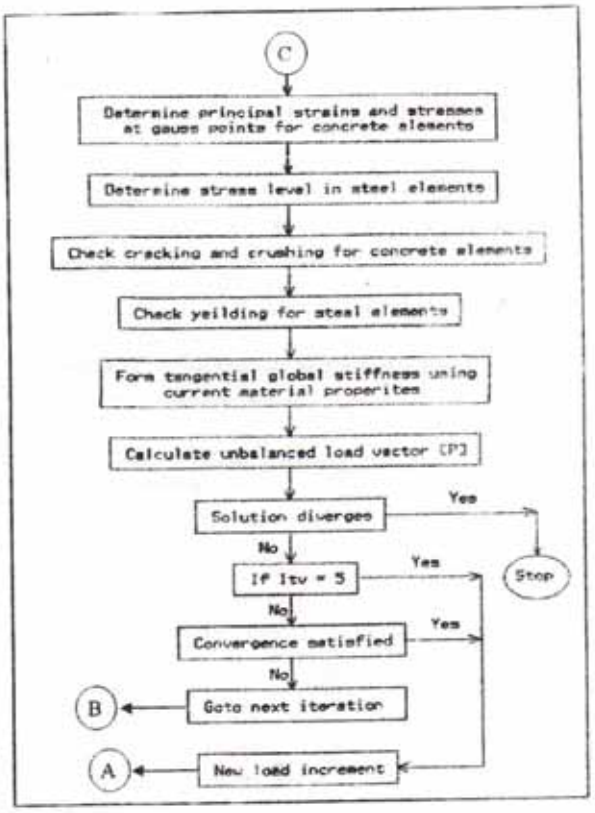

Flow chart for the nonlinear algorithm

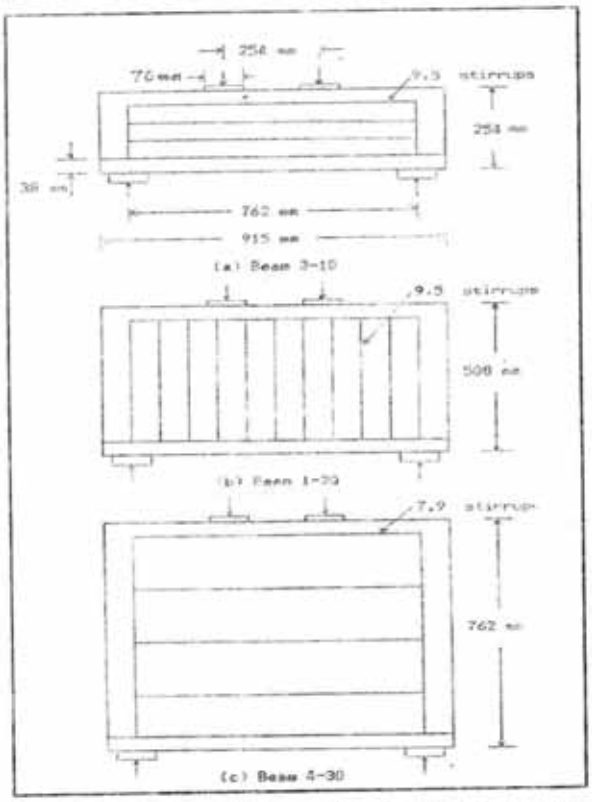

Fig. (3) Detaila of Beams Tested by Kong[13].

5.1.2 Analytical results

The Fig.(5) shows comparison between analytical and experimental load-deflection curves and Table (2) gives failure loads for beams 3-10, 1-20 and 4-30 using different models. From the above figure and table it's obvious that the simulation of the support has a significant effect on behavior of the three beams, especially on the beams 1-20And 4-30. The ultimate load was increased from 97 % to 104.1%, from 53% to 82.4%, and 44.6% to 74.2% of the experimental ultimate load for the beams 3-10, 1-20 and 4-30, respectively. Although by simulation of the support. the ultimate load or the beams3-10, 1-20, and 4-30 was increased. But these beams failed Locally by crushing of the concrete above the support.

This is especially for beam 4-30, where the crushing occurred before occurrence of any diagonal cracks in the shear zone. Therefore, an extra reinforcement was provided in beams 1-20. and 4-30, where three vertical bars or 6.4 mm (1/4 in) was provided in middle and two sides of the elements under the load and above the support.

The final crack pattern for beams 3-10, and 4-30 are shown in Fig (6). The cracking in all beams started in flexural zone. At the load 66.75 KN. in beam 1-20, and 378.25 KN in beam 4-30 diagonal cracks between the load and the support were initiated. The final analytical cracks patterns for beams 3-10 and 4-30 show good correlation with experimental one both in distribution and orientation.

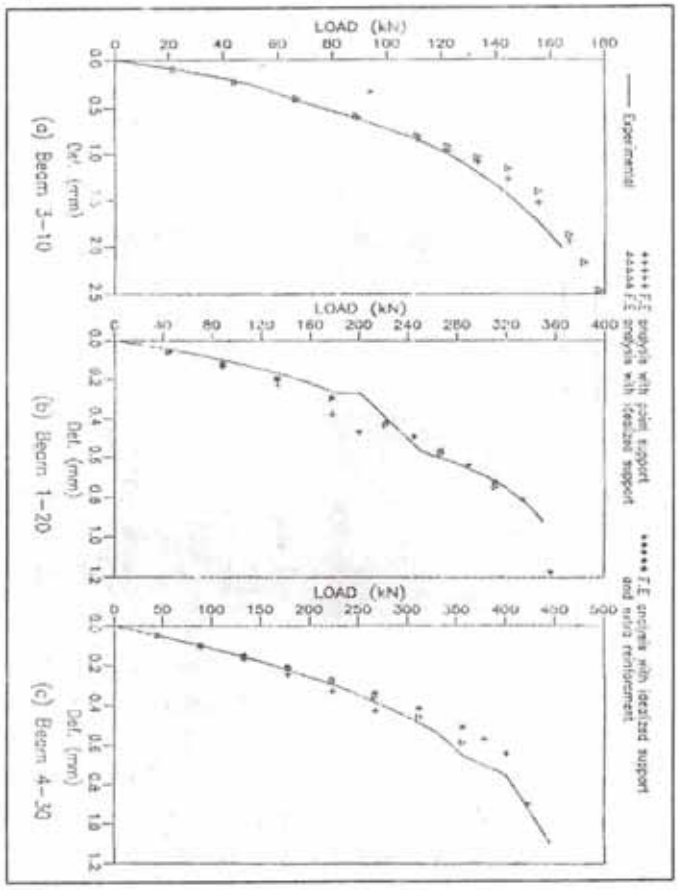

Fig. (5) Load – Deflection curves for beoms 3-10, 1-20, and 4-30

Table (2) Failure loads for beams of Kong [8] using different models

Beam No.	Experimental kong[8] (KN)	Model of Ref.[13] (KN)	The proposed model (KN)		
			Point support	Idealized support	Idealized support with extra reinforcement
3-10	171	178.00	166.00	178.0	*
1-20	380	400.50	200.25	311.5	356.00
4-30	480	467.25	267.00	356.0	422.75

* Extra reinforced was not used in beams 3-10.

5-2 Reinforced Concrete Deep Beams With Openings

The Finite element program is applied to solve deep beams with openings. The analyzed beams were obtained from beam 1-20 by removing the web reinforcement, and putting openings with different locations in the shear span. A total of six deep beams with openings were obtained. Details of these beams are shown in Fig (7). The concrete in all these beams is idealized by using 25 elements (5 elements along the half-span and 5 elements along the depth (see Fig (8)).

5-2.1 Analytical results

Analytical final crack patterns for beams 1-20-1 to 1-20-6 are shown in Fig. (8). The first cracks, which are marked by points, appeared at the load 89 KN in all beams except in beam 1-20-4, where the first cracks occurred at the load 44.5 KN.

Fig.(9) shows effect of the openings on behavior of beam 1-20-1. From this figure, it is clear that presence of the openings in the beam decreased its stiffness. Hence the ultimate load capacity is decreased, and the deflection is increased. Among beams 1-20-1 through 1-20-6 the beam 1-20-1 (with no openings) have the maximum ultimate load, while the beam 1-20-4 (with openings near the supports) has the minimum ultimate load.

One can notice also the early diagonal cracks at corners of the openings as a results of stress concentration. Presence of horizontal cracking at the top left corner of the openings is noticed in beams 1-20-2, 1-20-3 and 1-20-6.

5.2.2 Comparison between behavior of beam 1-20-1 and beam 1-20-2

A comparison between behavior of beams 1-20-I (with no openings) and I-20-2 (with openings near the mid-depth in shear zone) is presented here to study effect of these openings on the distribution of concrete stress.

5.2.2.1 Lateral stress (fx)

The variation of lateral stress (fx) along the beam depth of beams I-20-I and 1-20-2 at mid span section, and at distance of 0.5 D from the support are shown in Figs. (10) to (13). It is clear from these figures that presence of openings made a dramatic change in nature of the distribution (Fig (11) and (13)). The discontinuous part of these curves are due to cracking of concrete in these regions. In Figs. (10) and (12), it is shown that the neutral axis has to be moved upward as load is increased due to concrete cracking in the tension zone, while this is not true for Fig. (13) because the cracking is also occurred at the mid depth adjacent to the opening.

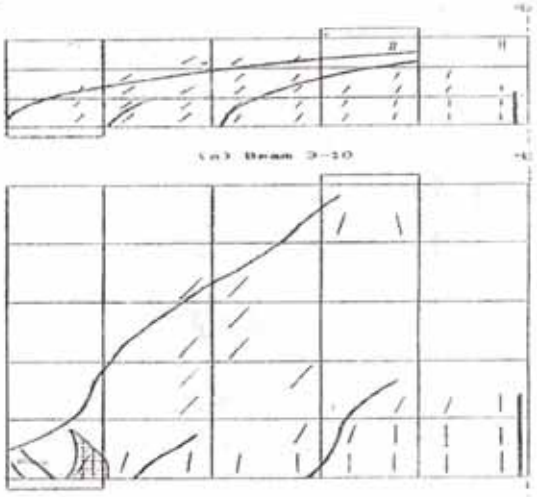

(B) Beam 4-30

Single lines indicate analytical cracks.
Double lines indicate analytical crushing.
Represents experimental crushing.

Fig. (6) Analytical and experimental crack patterns at failure load for beams 3-10 and 4-30

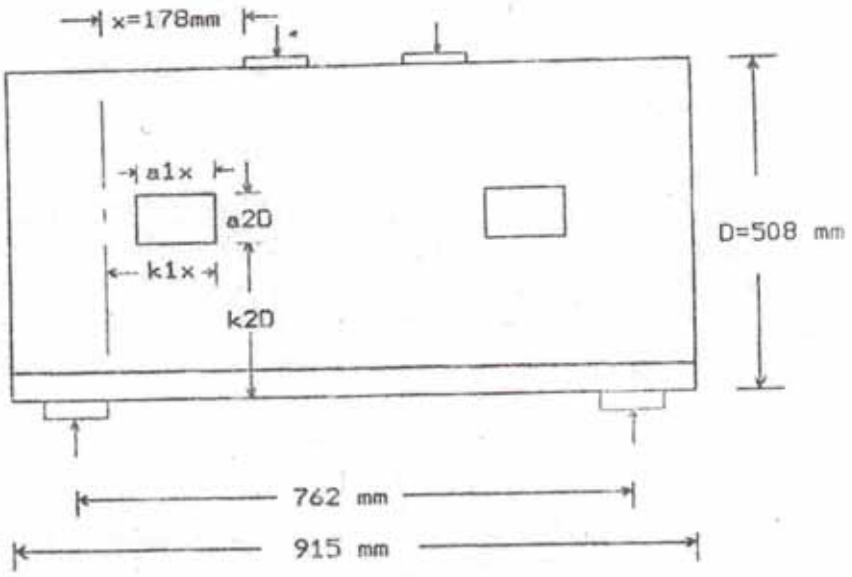

Ref. No. of beams	size		position	
	a1	a2	k1	k2
1-20-1	---	---	---	---
1-20-2	1	0.185	1	0.445
1-20-3	1	0.185	1	0.630
1-20-4	1	0.185	1	0.260
1-20-5	0.5	0.185	1	0.445
1-20-6	0.5	0.185	0.5	0.445

Fig.(7) Refrence No.s, sizes, and positions of the openings in beams 1-20-1 through 1-20-6

Failure load=311.5 kN

(a) Beam 1-20-1

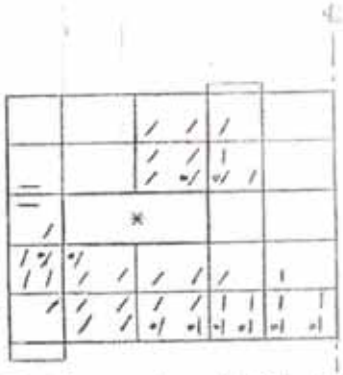

Failure load=200 kN

(b) Beam 1-20-2

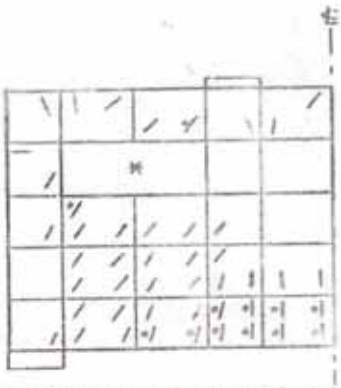

Failure load=200 kN

(c) Beam 1-20-3

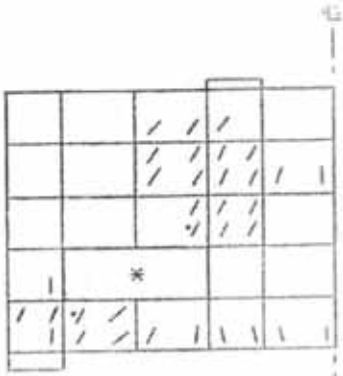

Failure load=133.5 kN

(d) Beam 1-20-4

Failure load=267 kN

(e) Beam 1-20-5

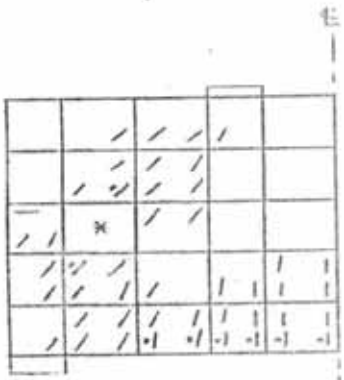

Failure load=267 kN

(f) Beam 1-20-6

* indicates opening position.

Fig. (8) Crack paterns at failure for beams 1-20-1 through 1-20-6

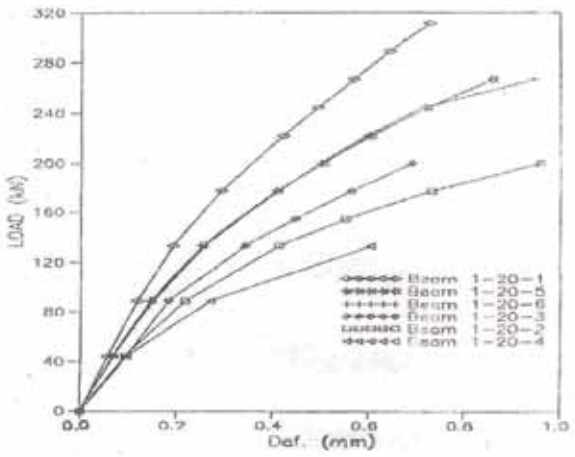

Fig. (9) Opening effect on the behavior of Beam 1-20

5.2.2.2 Vertical stresses

The vertical stress variation along the half span of beams 1-20-1 and 1-20-2 at a distance of 0.76 D from the extreme top fiber are shown in Figs. (14) and (15). In beam 1-20-1 the distribution of vertical stress at the first load increment 44.5 KN varies from maximum above the support to minimum at the centerline, while in beam 1-20-2 the distribution is different for the same load. This can be attributed to presence of openings in beam 1-20-2, For the subsequent load increments, it can be seen that in both beams there is some kind of stress concentration at the points marked by "c". This is because these points have been cracked, and the stress in cracked direction reduce to zero, consequently the state of stress become uniaxial.

5.2.2.3Shear stresses

The shear stress variation along the depth of beams 1-20-1 and 1-20-2 at distance 0.21D, from support (nearly at middle of the shear span) are shown in Figs. (16) and (17).

The shear stress distribution for beam 1-20-1 is parabolic in all loading stages, While beam 1-20-1 the distribution curve in each load is divided, into two nearly parabolic curves. In each curve (Fig (17)) the shear stress reduced to zero at the upper and lower boundaries of the openings. which is logically true because the shear stress is equal to zero at the lower and upper faces of the opening.

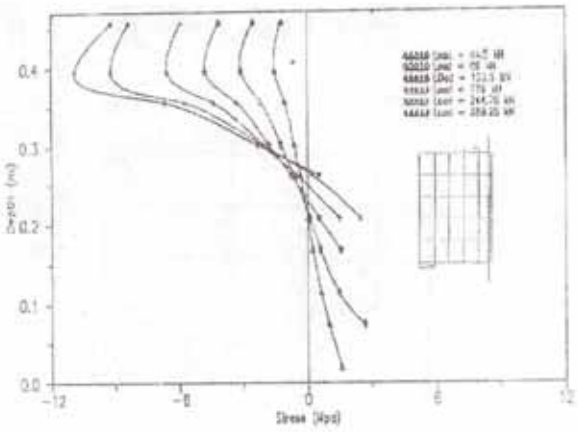

Fig.(10) Stress (Tx) variation along the depth of Beam 1-20-1 at midspan section under different loading stages

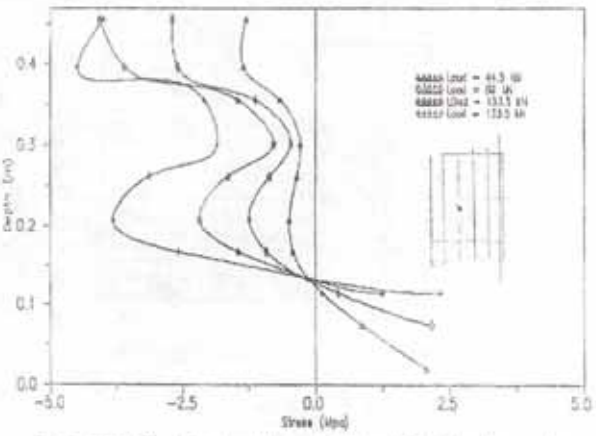

Fig.(11) Stress (Tx) variation along the depth of Beam 1-20-2 at midspan section under different loading stages

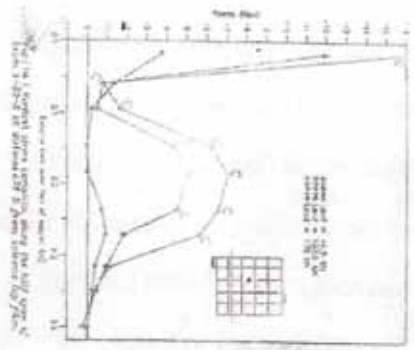

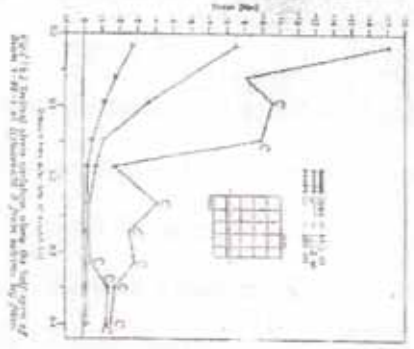

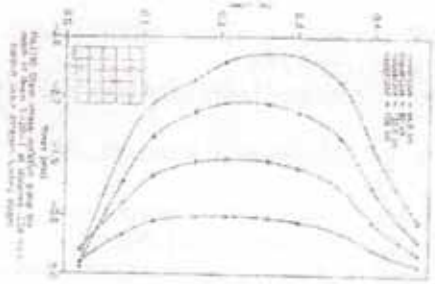

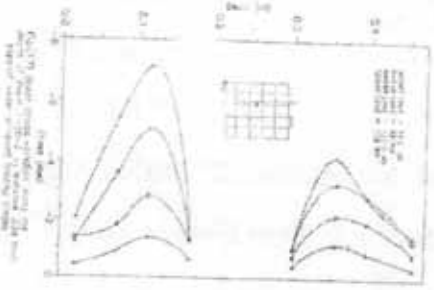

5.2.2.4 Comparisons

From table (2), it is clear that failure loads for beams 3-10, 1-20, and 4-30 were found to be 104.1%, 94.1% and 88.1% with respect to Kong's experimental results, respectively. While Mahmood's results were 104.1 %, 105.95 % and 97.34% with respect to Kong's results, respectively. The above discrepancies are mainly due to that a trial-proportioning of reactions at the supported nodes was used in Mamoond's investigation. While in our investigation a discretized attached base-plate and an extra reinforcement above the support and under the load were used moreover once steel elements yielded; they were cancelled for the next loading stage in forming the stiffness matrix of the domain.

6- Conclusions

1. The present nonlinear solution algorithm for the analysis of reinforced concrete deep beams with or without openings can be used to predict the behavior of deep beams in certain aspects.
2. The finite element method can predict to a large extent the behavior and failure load with the presence of openings in the beams and deep beams.
3. The proposed finite element model gives a good representation for the deep beams behavior.
4. The constitutive relations for concrete proposed by Liu [17] were found to be satisfactory and reliable to use for deep beams.
5. The smeared cracking model can represent the real cracking process in deep beams.
6. The simulations of supports, and provision of extra reinforcement under the load and above the supports have a significant effect on the analytical behavior of deep beams, especially for beams with span depth ratio less than 2. This conclusion about simulation of supports was also stated by Mahmood [13].

Acknowledgements

The writers wish to thank the Department of Civil Engineering, College of Engineering, University of Salahadden, where this Investigation was made.

References

1. Hasan S. A., (Finite Element Analysis of reinforced Concrete Deep beams). M.Sc. Thesis, September 1994, University or Salabaddin. Arbil-Iraq.
2. ACI Committee 318. (Building Code Requirement for Reinforced Concrete) . (ACI 318-83) ACI. Detroit.
3 Ngo. D. and Scordelis, AC. (Finite Element Analysis or Reinforced Concrete Beams). *ACI Jour., Proc.* Sep. 1968, **64**(9), 757-766.
4. Nilson. A.H. (Nonlinear Analysis or Reinforced Concrete by Finite Element Method*), ACI Jour., Proc.,* Sep. 1968, **65**(9) 757-766.
5. Valliappan. S.. and Doolan. T.F.. (Nonlinear Stress Analysis of Reinforced Concrete). *ASCII Proc..* Jour. of the Struct. Div.. April 1972, **98**(4), 885-897.
6 Robins, P.J. and Kong. F.K. (Modified Finite, Element Method Applied to Reinforced Concrete Deep beams). *Civ. Eng. and pub. works Rev.*, Nov. 1973, **68**(808) 963-966.
7. Suidan, M. and Sehnobrich. W.C.,(Finite Element Analysis of Reinforced Concrete). *ASCE Proc., Jour. of the Struc. Dlv.*, Vol.99, No ST10, Oct. 1973, pp. 2109-2122.
8. Kong. F.K Robins. P.J.. and Cole. D.F.. (Web Reinforced Effects on Deep Beams). ACI Jour., Proc., Vol. 67, No. 12. Dec. 1970. pp 1010-1017.
9. Phillips. D.V, and Zienkiewicz. O.C.. (Finite Element Non-linear Analysis of Concrete structures). *Proc. of ICE. part 2.* March 1976, 61,59-88.
10. Cope. R.J. and Rao. P.. (Nonlinear Finite Element Analysis of Reinforced Concrete Slab Structures). *Proc. of ICE, part 2.* March 1977, 63, 159-119.
11. Cedolin. L.. and Die Poli. S. (Finite Element Studies of Shear-critical R/C Beams). *ASCE. Proc.. Jour. of Eng. Mech. Div.*, March 1977 ,103. No. Em3, 395-410.
12. Gogate. A.B., and Bishara, A.G.. (Finite Element Analysis of Deep Beams). *Indian Concrete Journal*, Dec. 1980,**54**(12),326-333.
13. Mahmood, M.N., (Nonlinear Finite Element Analysis of Reinforced Concrete Deep Beams), M.Sc. Thesis. Junary 1986. University of Mosul.
14 Kotsovos, M.D., (Behavior or Reinforced Concrete Bems with a Shear span to Depth Ratio between 1 and 25), *ACI Jour.. Proc.*, May-June 1994, **81**(3), 279-286.
15. Kupfer, H.. Hildsdorf. H.K. and Rusch. H., (Behavior of Concrete Under Biaxial Stresses). *ACT Jour.. Proc.* August 1969, **66**(8) 656-666.
16. Kupfer. H.. and Grestle, K.H., (Behavior or Concrete Under Biaxial stresses*). ASCE. Proc.. Jour. of Eng. Mech. Dlv.*, Aug. 1973, EM4., 852-866.
17 Liu. T.C.Y, Nilson, A.H, and Slate. F.O, (stress-Strain Response and Fracture or Concrete in Uniaxial and Biaxial Compression), *ACI Jour., Proc..* May 1972, **69**(5), 291-295.
18. Liu, T.C.Y. Nilson, A.H. and Slate, F.O, (Biaxial Stress-strain Rotations for Concrete). *ASCE. Proc.. Jour. of the Struct. Div..* May 1972, 98: No. STS.. l025-1034.
19. Tasuji, M,E. Nilson, A-H. and Slate, F.O., (Stress-Strain Response And Fracture or Concrete in Biaxial Loading). *Aci. Jour,. Proc..* July 2978, **75**(7), 306-312.
20 Tasuji. M.E. Nilson, A-H.. and Slate. F.O., (Biaxial Stress-strain Relationships for Concrete), *Mag. of Concrete Research.* Dec. 1979, **31**(l09), 218-224.
21 Huebner. K.H, and Thonton, E.A..(The Finite Element Method for Engineers), and Edition, John Wiley & sons, Inc., Inc.. New York. 1982.
22. Ziankiewlcz. O.C, (The Finite Element Method in Engineering Science). 2nd Edition. McGraw-Hill. London, 1971.
23. Cook. R.D., (Concepts and Application of Finite Element Analysis), 2nd Edition. John Wiley & Son's, Inc.. New York. 1981.
24. Cheung. Y.K.. and Yeo. M.F.. (A practical Introduction to Finite Element Analysis), Pitman Publishing Ltd, Great Britain, 1979.
25. Dodds. R.H. Darwen. D., and Leibengood, L.D.. (Stress Controlled Smeared Cracking in R/C Beams). *Asce. Proc., Jour. or Struct. Div..* Sep. 1984, **110**(9),1959-l979.
26. Bedard. C., and Kotsovos, M.D., (Application of NLFEA to Concrete Structures), *ASCE. Proc.. Jour. of Struct. Div..* Dec 1985, **III**(12) 2691-2705.
27. Kotsovos. M.D., (Behavior of Reinforced Concrete Beams with a Shear span to Depth Ratio Between 2.5 and 5). *ACI Jour.. Proc..* Nov.-Dec. 1986, **83**(3) 1026-loa4.

شیکاری نێرگەی کۆنکرێتی قوواڵی شیش دار بە رێی ئەندامە دیاری کراوەکان

محمد محمود احمد

سەرکەوت اسعد حسن

کۆلیجی ئەندازیاری/ زانکۆی سەلاحەدین / هەولێر – هەرێمی کوردستان - عێراق

کورتە

لەم لێکۆڵینەوەیەدا شیکاری جۆری ناڕاستەوخۆ کراوە بۆ ئەندامی نێرگەی کۆنکرێتی قوواڵی شیش دار بە بەکارهێنانی رێی ئەندامە دیاریکراوەکان، بۆ ئەوەی ڕەوشتی ئەو جۆرە ئەندامانە بەپێی سیفەتەکانی کە سەرئەنجامی ئەرکی دوو تەوەرەیی و درزبردن و وراوخاش بوون و ، توانایی کۆنکرێتەکە بۆ خۆڕاگریی لەبەردەم هێزی بڕین پاش ڕووداندی درزەکان وە ملکەچکردنی شیشەکان لەژێر باردا بخەملێندرێت.

کۆنکرێت لەم لێکۆڵینەوەیەدا پێشان دراوە وەکو ئەندامێکی چوارلای –هەشت خاڵی، وە شیش بە ئەندامی یەک لای دووخاڵ پێشان درا کە پەیوەندیداری ڕاستەوخۆ بە گرێکانی ئەندامە هاوسێکانی کۆنکرێتیەکەوەیە.

ئەو ئەنجامانەی دەست کەوت لە شیکارکردنەکەدا زۆر نزیک بوو لە ئەنجامی تری هاوشێوە کە لە تاقیگەدا بەدەست هاتبوون، پاش ئەوە ڕێگا شیکارییەکە بەکارهات بۆ شیکارکردن، بۆ ئەو نێرگە کۆنکرێتە قووڵە شیشدارانەی کە لەشوێنی جیاجیادا، کونی جۆراوجۆری تیدابوو، بۆ مەبەستی زانینی کاریگەری ئەو کونانە لەسەر کەمکردنەوەی توانای خۆڕاگری بەرامبەر بە بار، وە چۆنیەتی بڵاوبوونەوەی درزەکان، وە ئەرک لەسەر هەر خاڵێک.

تحليل العتبات الخرسانية العميقة المسلحة بطريقة العناصر المحددة

محمد محمود احمد
سەركەوت اسعد حسن
كلية الهندسة/ جامعة صلاح الدين/ اربيل / أقليم كردستان - العراق

الخلاصة

يتناول هذا البحث التحليل اللاخطي للعتبات الخرسانية المسلحة العميقة بإستخدام طريقة العناصر المحددة. إن التحليل اللاخطي تضمن السلوك اللاخطي للخرسانة، وعدم تجانس خواصها نتيجة للاجهادات الثنائية المحور، تشقق وتهشم الخرسانة، قابلية الخرسانة على تحمل قوى القص بعد حصول التشققات، وخضوع حديد التسليح.

تم تمثيل الخرسانة بعناصر رباعية متطابقة الدالة ذات العقد الثمانية (Quadrilateral isoparametric eight-noded elements). أما حديد التسليح الرئيسي والثانوي فقد تم تمثيله باستخدام عناصر أحادية المحور مرتبطة بصورة مباشرة مع عقد الخرسانة.

تم إختبار مدى ملائمة النموذج المقترح عن طريق تحليل ثلاثة عتبات خرسانية مسلحة عميقة. النتائج التي تم الحصول عليها أعطت تطابقا جيدا مع النتائج العملية. تم تحليل عتبات خرسانية مسلحة عميقة أخرى حاوية على فتحات مختلفة الأحجام والمواقع لمعرفة مدى إمكانية النموذج المقترح لتمثيل وجود الفتحات. النتائج التي تم الحصول عليها بينت أن النموذج قادر على تمثيل مثل هذه المسائل من حيث تأثير هذه الفتحات على سعة التحمل الأقصى، إنتشار التشقق، توزيع الإنفعالات والإجهادات في العتبات.

Received 16/5/2000
Accepted 5/9/2000

وەرگیرا لە ٢٠٠٠/٥/١٦
پەسەند کرا لە ٢٠٠٠/٩/٥ دا